

## Correlation between Magnetism and Spin-Dependent Transport in CoFeB Alloys

P. V. Paluskar,\* R. Lavrijsen, M. Sicot, J. T. Kohlhepp, H. J. M. Swagten, and B. Koopmans  
*Department of Applied Physics, cNM, Eindhoven University of Technology, 5600 MB, The Netherlands*  
 (Received 12 June 2008; published 7 January 2009)

We report a correlation between the spin polarization of the tunneling electrons and the magnetic moment of amorphous CoFeB alloys. Such a correlation is surprising since the spin polarization of the tunneling electrons involves *s*-like electrons close to the Fermi level ( $E_F$ ), while the magnetic moment mainly arises due to all the *d* electrons below  $E_F$ . We show that probing the *s* and *d* bands individually provides clear and crucial evidence for such a correlation to exist through *s-d* hybridization, and demonstrate the tunability of the electronic and magnetic properties of CoFeB alloys.

DOI: 10.1103/PhysRevLett.102.016602

PACS numbers: 72.25.Mk, 75.50.Kj, 85.75.-d

At the very foundation of spintronics lie the facts that the conduction electrons in transition metal ferromagnets possess high mobilities and that they get highly spin polarized as a consequence of their interaction with localized *d* electrons [1]. In magnetic tunnel junctions, these *s*-like electrons dominate the tunneling current and are primarily responsible for the tunneling magnetoresistance effect [2,3]. Early experiments to measure the spin polarization of these tunneling electrons (TSP) in  $\text{Ni}_{1-x}\text{Fe}_x$  alloys yielded the unexpected result that the alloy magnetic moment ( $\mu_{\text{alloy}}$ ) as well as their TSP displayed the Slater-Pauling (S-P) behavior [4]. The S-P behavior of  $\mu_{\text{alloy}}$  [see Fig. 1(a)] is the well-known deviation from a linear change resulting in a maximum [5,6] as the alloy composition changes. While this nonmonotonic behavior of  $\mu_{\text{alloy}}$  is commonly observed in transition metal compounds, their TSP exhibiting a similar curve is very surprising. This surprise stems from the fact that, while  $\mu_{\text{alloy}}$  is an integral over all states below the Fermi level ( $E_F$ ) and is dominated by *d* electrons, the TSP originates from transport of *s*-like electrons close to  $E_F$ . This correlation has been observed only occasionally in experiments [7–10]. However, the understanding of such a correlation has been neither experimentally nor theoretically addressed, making it a fundamental, long-standing, and highly debated issue. Moreover, the existence of such a correlation between  $\mu_{\text{alloy}}$  and TSP will allow the engineering and tuning of magnetic and electronic properties of ferromagnetic alloys for application in spintronics. We believe that the key to understand this correlation is a combined study of the element-specific *d*-band electronic structure and the *s* electron dominated TSP in a perceptively chosen material.

In this Letter, we demonstrate the S-P behavior of both the TSP and  $\mu_{\text{alloy}}$  of amorphous  $\text{Co}_{80-x}\text{Fe}_xB_{20}$  alloys. The measured curves of both these properties show distinct similarity in trend and provide an undisputable hint to this correlation. Together with an intuitive understanding of the correlation, we also report a detailed insight into the various aspects of  $\text{Co}_{80-x}\text{Fe}_xB_{20}$  electronic structure. CoFeB alloys are specifically chosen for the following

reasons. (i) Being amorphous, they are highly insensitive to the miscibility of their constituents. (ii) Contrary to most crystalline alloys, their atomic structure does not undergo structural transitions with their composition on the microscopic scale. Both the above distinctions allow easy experimental access to their characteristic properties. (iii) Given their unquestionable importance in spintronics today [11,12], and their complex ternary amorphous nature, a comprehensive effort to understand their intrinsic properties remains to be embarked upon.

Since the basic mechanisms for this correlation must involve the electronic structure of the *d* bands, we use x-ray absorption (XAS) and magnetic circular dichroism (XMCD) to probe their properties. These techniques demonstrate a direct observation of the S-P behavior for the orbital ( $m_o$ ) and spin ( $m_s$ ) moments, as well as the expected changes in the exchange splitting ( $\Delta_{\text{ex}}$ ). Together, the observations of the S-P behavior of  $m_o$ , and the S-P behavior of  $m_s$  and  $\Delta_{\text{ex}}$ , provide strong evidence to establish that the alteration of the electronic structure with changing alloy composition is, through *s-d* hybridization, primarily responsible for the correlated behavior of  $\mu_{\text{alloy}}$  and TSP. We would also like to emphasize that such a clear observation of the S-P behavior, a characteristic of most transition metal ferromagnetic alloys, has not been established yet using the XMCD technique. Moreover, with this dem-

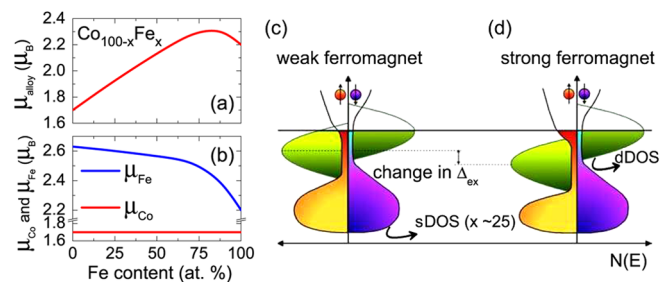


FIG. 1 (color online). Schematic representation of the S-P behavior for  $\text{Co}_{100-x}\text{Fe}_x$ : (a) S-P curve of  $\mu_{\text{alloy}}$  [5]. (b) Known trend of the element-specific Co and Fe moments [6]. DOS of (c) weak and (d) strong ferromagnets.

onstrated tunability and insight into their magnetic, electronic, and transport properties, we believe that CoFeB alloys open several new possibilities to engineer and enhance the performance of spin-torque devices.

Sample preparation and measurement techniques are discussed in the supplementary material [13]. A schematic representation of the S-P curve is exemplified for  $\text{Co}_{100-x}\text{Fe}_x$  alloys in Fig. 1(a) as a function of the Fe content. Notice that the generic shape for the total magnetic moment is simply a concentration-weighted average of element-specific moments of Co and Fe shown in Fig. 1(b). As sketched in the density of states (DOS) of Fig. 1(d), Co is a strong ferromagnet with its spin-up  $d$  band completely filled. Quite generally, as the alloy composition changes, its electronic structure and its moment remain unaffected [5] [see Fig. 1(b)]. On the contrary, Fe being weakly ferromagnetic with both spin  $d$  bands only partially filled [see Fig. 1(c)] shows a substantial increase in moment as the Fe content decreases [see Fig. 1(b)]. Eventually Fe undergoes a crossover from weak to strong ferromagnetism [see Figs. 1(c) and 1(d)]. Note that this crossover of Fe with the associated increase in the Fe moment essentially causes the S-P behavior of  $\mu_{\text{alloy}}$  [5,6].

One may ask whether amorphous CoFeB alloys also show the S-P behavior. First-principles electronic structure calculations predict weak ferromagnetism in amorphous  $\text{Fe}_{80-x}\text{B}_x$  alloys [14] and strong ferromagnetism in amorphous  $\text{Co}_{80-x}\text{B}_x$  alloys [15]. Thus, one may expect that as the Fe content decreases, the Fe DOS undergoes a transition from weak to strong ferromagnetism, which would cause the S-P behavior. Just as expected, measured using a superconducting quantum interference device (SQUID), Fig. 2(a) shows that  $\mu_{\text{alloy}}$  of  $\text{Co}_{80-x}\text{Fe}_x\text{B}_{20}$  exhibits the S-P curve. Such a curve has also been measured before [16]. Next, we focus on CoFeB TSP and the changes in the alloy electronic structure which affect it.

The magnitude of the TSP measured using superconducting tunneling spectroscopy (STS) [3,17] is shown as open circles in Fig. 2(b). Notice that the change in  $\mu_{\text{alloy}}$  [Fig. 2(a)] over the whole composition range is around a factor  $\sim 1.7$ . Remarkably, the TSP too is observed to change by a very similar factor. While the observed correlation in the shape of the two measured curves is not perfect, this similarity between  $\mu_{\text{alloy}}$  and the TSP is puzzling since, as mentioned earlier,  $\mu_{\text{alloy}}$  evolves from  $d$  electrons while  $s$  electrons dominate tunneling through  $\text{AlO}_x$  [2,3]. Nevertheless, given this apparent correlation, if one naively assumes that the TSP and moment of Co and Fe in the alloy are the same as that in pure Co or Fe films, and that B is unpolarized [18], then one could estimate the alloy TSP using a simple linear concentration-weighted combination of the known moment and TSP values for pure Co and Fe [see Eq. (S1), supplementary material [13]]. The TSP values so estimated are shown as open squares in Fig. 2(b). One notes a striking similarity of this

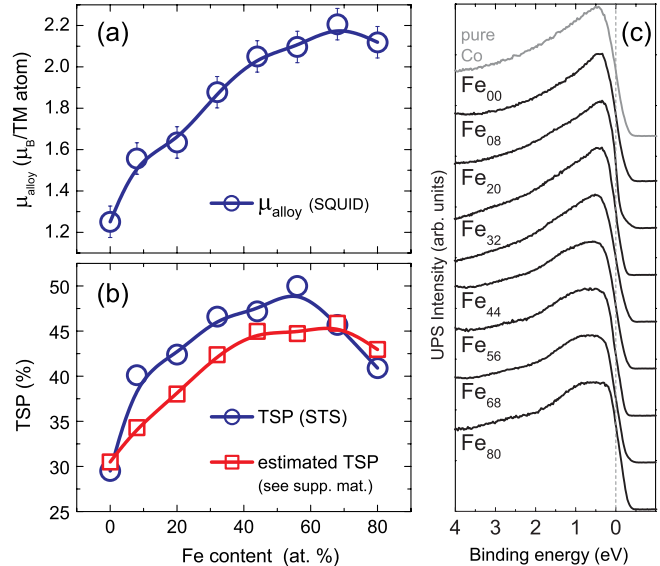


FIG. 2 (color online). (a)  $\mu_{\text{alloy}}$  measured with SQUID (b) TSP measured with STS and the estimated TSP (see supplementary material [13] and text below). (c) UPS data.

curve with the measured TSP as well as with  $\mu_{\text{alloy}}$ . In fact, the use of this *crude and admittedly oversimplified approximation* seemingly estimates the alloy TSP within  $\sim 5\%$  of its measured value. Given this oversimplified approximation, one may wonder whether bulk electronic and magnetic properties may be fit to describe electronic transport at the interface. However, as we have shown in our previous study [3], interface bonding effects at such a complex interface between an amorphous barrier and a chemically and structurally disordered ternary amorphous alloy are an average over the configuration space. In other words, at the interface, (i) the arrangement of each atomic species in the ferromagnet with respect to those of the oxide and (ii) the variation in the local coordination within the ferromagnetic alloy are expected to change from site to site. Consequently, though bonding may play a significant role *locally*, the effect of such bonding may average out over a macroscopic junction.

In order to get insight into the changes of the electronic structure which cause this correlation, we measured valence band spectra using ultraviolet photoemission spectroscopy (UPS) [see Fig. 2(c)]. A systematic and pronounced impact of the changing alloy composition on the valence band structure is seen in the spectra. The sharp peak around 0.5 eV for the Co-rich compositions broadens as the Fe content increases up to  $\text{Fe}_{56}$  and then levels off. Based on the behavior of  $\mu_{\text{alloy}}$ , we tentatively ascribe this pronounced spectral change to the gradual crossover from weak to strong ferromagnetism (see supplementary material [13]).

The UPS spectra provide clear and direct evidence of the systematic changes occurring in the electronic structure.

However, they are not element specific. Such an insight would be invaluable considering that the S-P behavior essentially derives from the changes in the Fe  $d$  DOS. Therefore, we performed XAS and XMCD at the Fe  $L_{2,3}$  edges using synchrotron radiation. Next, we discuss two aspects: (i) the orbital moment and (ii) the spin moment and exchange splitting. The changes in these properties are interrelated. They explicitly demonstrate the transition of Fe from weak to strong ferromagnetism together with the changes occurring in the DOS at  $E_F$ . Moreover, as we shall see later, this transition also provides a simple picture of a correlation between the  $s$  and  $d$  electrons.

Figure 3(a) shows isotropic XAS spectra with standard background subtraction (step function [19]). The difference in the absorption cross section measured for left or right circularly polarized ( $\sim 66\%$ ) light results in the corresponding XMCD spectra shown in Fig. 3(b). In Figs. 3(a)–3(d), note that Fe<sub>100</sub> represents pure Fe, while Fe<sub>0</sub> represents Co<sub>80</sub>B<sub>20</sub> measured at the Co  $L_{2,3}$  edges.

*Orbital moment ( $m_o$ ).*—According to Thole *et al.*,  $m_o$  is given by the orbital sum rule  $\frac{m_o}{n_{3d}} = \frac{4}{3} \frac{\Delta A_3 + \Delta A_2}{A_3 + A_2}$  [20]. As shown in Fig. 3(a), the integrated areas under the  $L_{2,3}$  edges of isotropic XAS spectra are used to extract  $A_{2,3}$ , while the corresponding areas under the XMCD spectra are used to extract  $\Delta A_{2,3}$  [see Fig. 3(b)].  $n_{3d}$  denotes the number of  $d$  holes, which are unknown for CoFeB.  $\frac{m_o}{n_{3d}}$  is plotted in Fig. 3(c). First, the absolute value of  $m_o$  measured for Fe<sub>100</sub> ( $\sim 0.13\mu_B$  with the known  $n_{3d} = 3.4$ ) agrees fairly well with the calculated value of  $\sim 0.1\mu_B$  [21]. Moreover, the curve in Fig. 3(c) resembles an inverted S-P curve and implies the quenching of  $m_o$  with increasing Fe content. We confirmed this quenching of  $m_o$  by analyzing other ratios known to be sensitive to the spin-orbit interaction (see supplementary material [13]). The changes in the Fe DOS sketched in Figs. 1(b)–1(d) may be shown to directly result in the observed quenching of  $m_o$ . It is known that  $m_o \propto [n^\uparrow(E_F) - n^\downarrow(E_F)]$ , where  $n^\uparrow(E_F)$  is the spin-resolved total DOS at  $E_F$  [21–23]. In other words,  $m_o$  is directly proportional to the “magnetic” DOS at  $E_F$ . A transition from strong to weak ferromagnetism [i.e., from Figs. 1(d) to 2(c)] where the spin-up band moves towards  $E_F$  would result in a decrease in  $n^\uparrow(E_F) - n^\downarrow(E_F)$ , consequently quenching  $m_o$ . Later we will see that these changes in the “magnetic” DOS at  $E_F$  may also affect the TSP.

*Spin moment ( $m_s$ ) and exchange splitting ( $\Delta_{ex}$ ).*—The change in  $n^\uparrow(E_F) - n^\downarrow(E_F)$  is expected to have a direct effect on  $m_s$  which constitutes  $\geq 90\%$  of the total moment. Figure 3(d) shows  $\frac{m_s}{n_{3d}}$  calculated using the spin sum  $\frac{2\Delta A_3 - 4\Delta A_2}{A_2 + A_3} - \frac{7\langle T_z \rangle}{n_{3d}}$  [24]. The magnetic dipole term ( $\langle T_z \rangle$ ) is neglected as its local contributions are expected to cancel out for an amorphous system [25]. First, the absolute value of  $m_s$  for Fe<sub>100</sub> ( $2.14\mu_B$  with  $n_{3d} = 3.4$ ) is in excellent agreement with the moment of pure Fe [21,22]. Most remarkably, the shape of  $\frac{m_s}{n_{3d}}$  is distinctly similar to that of

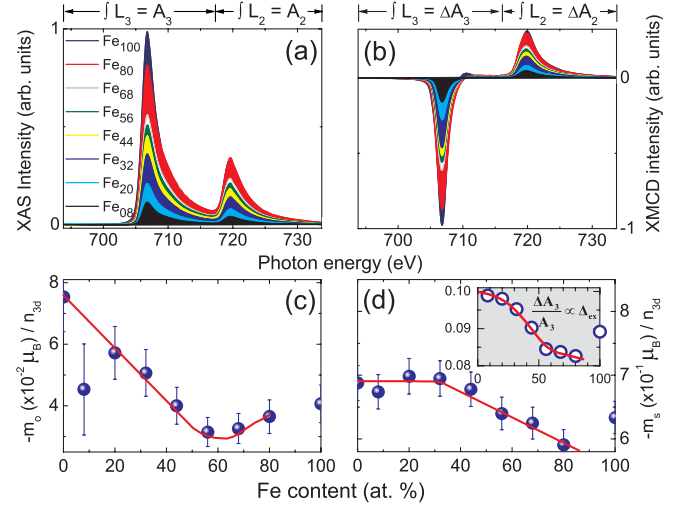


FIG. 3 (color online). (a) Background subtracted Fe  $L_{2,3}$  edge XAS. (b) Corresponding XMCD spectra. (c) Orbital moment per hole,  $\frac{m_o}{n_{3d}}$ . (d) Spin moment per hole,  $\frac{m_s}{n_{3d}}$ . Inset shows  $\frac{\Delta A_3}{A_3} \propto \Delta_{ex}$  [27]. Fe<sub>0</sub> represents Co<sub>80</sub>B<sub>20</sub> measured at the Co  $L_{2,3}$  edges. Lines in (c) and (d) are guides to the eye.

$\mu_{Fe}$  shown for Co<sub>100-x</sub>Fe<sub>x</sub> in Fig. 1(b). Recall that the shape of this curve in CoFe is associated with the transformation of Fe from a weak to a strong ferromagnet. The analogous behavior of  $\frac{m_s}{n_{3d}}$  in Fig. 3(d) demonstrates that, as expected, Fe in CoFeB also undergoes a similar transformation. Accompanying this increase in  $m_s$ , another signature of the S-P behavior would be a similar increase of  $\Delta_{ex}$  known to be directly proportional to  $m_s$  [26]. Such an increase in  $\Delta_{ex}$  would also endorse our above arguments about the shifting of the  $d$  bands [see Figs. 1(b)–1(d)] which influences the magnetic DOS at  $E_F$  and  $m_o$ . Now,  $\Delta_{ex}$  has been shown to be directly proportional to the  $\frac{\Delta A_3}{A_3}$  (and  $\frac{\Delta A_2}{A_2}$ ) ratio [27]. In the inset of Fig. 3(d), in agreement with the expected increase in  $\Delta_{ex} \propto m_s$ , the  $\frac{\Delta A_3}{A_3}$  ratio also increases. Furthermore, quantitatively speaking, in Fig. 1(b) the Fe moment in Co<sub>100-x</sub>Fe<sub>x</sub> alloys is seen to increase by  $\sim 23\%$ , i.e., from the nominal  $2.2\mu_B$  to  $\sim 2.6\mu_B$ . Remarkably, in CoFeB,  $m_s$  and  $\Delta_{ex} \propto \frac{\Delta A_3}{A_3}$  also increase by  $\sim 20\%$  and  $\sim 25\%$ , respectively [see Fig. 3(d)]. Similar to the increase in  $\frac{\Delta A_3}{A_3}$ , we observe an increase in the  $\frac{\Delta A_2}{A_2}$  ratio (not shown). The absolute numbers for these ratios are also in very good agreement with [27].

Given this crossover of Fe from weak to strong ferromagnetism, we will now address how exactly these changes in the Fe  $d$  bands bring about the S-P behavior of the  $s$  electron dominated TSP. A clear indication comes from two independent arguments:

(i) Isomer shifts essentially probe the changes in the  $s$  electron charge density at the nucleus. In amorphous Co<sub>80-x</sub>Fe<sub>x</sub>B<sub>20</sub> these isomer shifts also exhibit the S-P

behavior [28] due to  $s$ - $d$  hybridization. Although these measured changes in the charge density represent all  $s$  electrons below  $E_F$  and are not spin resolved, they directly point to the interplay between  $s$  and  $d$  electrons.

(ii) The spin-resolved information is observed in our measurements where the S-P-like changes in  $m_o$ ,  $m_s$ , and  $\Delta_{\text{ex}}$  provide a direct insight into the underlying mechanism which causes a change in the TSP. More specifically, it is well-known that, due to  $s$ - $d$  hybridization, the  $s$  DOS is suppressed in regions of large  $d$  DOS [3] [see Figs. 1(c) and 1(d)]. As the Fe  $d$  bands cross over from weak to strong ferromagnetism, the spin-up  $d$  band gradually moves below  $E_F$ . Recall that this shift in the  $d$  band also resulted in the quenching of  $m_o \propto [n^\uparrow(E_F) - n^\downarrow(E_F)]$ . As shown in Fig. 1(c), due to this shift in the  $d$  bands, one may also expect an associated increase in the spin-up  $s$  electron DOS at  $E_F[n_s^\uparrow(E_F)]$ . This consequently increases the spin polarization of the Fe  $s$  electrons defined as  $P_s^{\text{Fe}} = [n_s^\uparrow(E_F) - n_s^\downarrow(E_F)]/[n_s^\uparrow(E_F) + n_s^\downarrow(E_F)]$ . As a result,  $P_s^{\text{Fe}}$  behaves in a manner similar to the magnetic moment of Fe in Fig. 1(b). The alloy spin polarization ( $P_s^{\text{alloy}}$ ) will consequently show the S-P behavior. Note that this increase in  $P_s^{\text{alloy}}$  will result in a corresponding increase in TSP, since the TSP is a good representative of  $P_s^{\text{alloy}}$  for these amorphous ferromagnets [3]. Here we assume that  $P_s^{\text{Co}}$  remains unchanged just like the Co moment in Fig. 1(b). We verified that the Co moment indeed remains unchanged using Co edge XMCD (see Fig. S6, supplementary material [13]).

Given this information on CoFeB electronic structure and the coherent picture for the existence of a correlation between  $\mu_{\text{alloy}}$  and TSP, the discrepancy with the TSP measurements on  $\text{Co}_{100-x}\text{Fe}_x$  alloys compiled from literature, which do not seem to exhibit the S-P behavior, may seem particularly puzzling. However, these alloys are crystalline and undergo structural transitions ( $\text{bcc} \leftrightarrow \text{fcc}$ ) depending on their compositions, which affect their electronic structure and may obscure a clear insight. Moreover, no composition dependent study which directly focuses on the structure, magnetism, and TSP of  $\text{Co}_{100-x}\text{Fe}_x$  alloys has been reported, nor any detailed XMCD measurements have been performed. On the contrary, the TSP of Co and Fe alloyed with Ru and V [7] is known to exhibit a correlation with  $\mu_{\text{alloy}}$ . XMCD measurements on these alloys could provide more understanding.

In summary, we investigated the magnetism and TSP of amorphous  $\text{Co}_{80-x}\text{Fe}_xB_{20}$  films. We find that the S-P behavior of the  $\mu_{\text{alloy}}$  is also seen in the  $s$  electron dominated TSP. XMCD data show a crossover from weak to strong ferromagnetism in the Fe DOS. To the best of our knowledge, this is the first observation of the S-P behavior in transition metal alloys using the XMCD technique. We conclude that this crossover in the Fe DOS, together with  $s$ - $d$  hybridization, provides an intuitive understanding of the direct correlation between  $\mu_{\text{alloy}}$  and TSP.

We thank NanoNed, a Dutch nanotechnology program of the Ministry of Economic Affairs, and STW-VICI for financial support and the staff of station 5U.1 at Daresbury labs, particularly Dr. T. Johal, for technical support.

\*p.v.paluskar@tue.nl

- [1] C. Chappert, A. Fert, and F. Nguyen, *Nature Mater.* **6**, 813 (2007).
- [2] S. Yuasa, T. Nagahama, and Y. Suzuki, *Science* **297**, 234 (2002).
- [3] P. V. Paluskar *et al.*, *Phys. Rev. Lett.* **100**, 057205 (2008).
- [4] R. Meservey, D. Paraskevopoulos, and P. M. Tedrow, *Phys. Rev. Lett.* **37**, 858 (1976).
- [5] R. Richter and H. Eschrig, *Phys. Scr.* **37**, 948 (1988).
- [6] M. F. Collins and J. B. Forsyth, *Philos. Mag.* **8**, 401 (1963).
- [7] C. Kaiser, S. van Dijken, S.-H. Yang, H. Yang, and S. S. P. Parkin, *Phys. Rev. Lett.* **94**, 247203 (2005).
- [8] A. T. Hindmarch, C. H. Marrows, and B. J. Hickey, *Phys. Rev. B* **72**, 100401 (2005).
- [9] C. Kaiser, A. F. Panchula, and S. S. P. Parkin, *Phys. Rev. Lett.* **95**, 047202 (2005).
- [10] D. J. Monsma and S. S. P. Parkin, *Appl. Phys. Lett.* **77**, 720 (2000).
- [11] A. A. Tulapurkar *et al.*, *Nature (London)* **438**, 339 (2005).
- [12] H. Kubota *et al.*, *Nature Phys.* **4**, 37 (2008).
- [13] See EPAPS Document No. E-PRLTAO-102-001902 for supplementary material. For more information on EPAPS, see <http://www.aip.org/pubservs/epaps.html>.
- [14] J. Hafner, M. Tegze, and Ch. Becker, *Phys. Rev. B* **49**, 285 (1994).
- [15] H. Tanaka *et al.*, *Phys. Rev. B* **47**, 2671 (1993).
- [16] R. C. O'Handley, R. Hasegawa, R. Ray, and C.-P. Chou, *Appl. Phys. Lett.* **29**, 330 (1976).
- [17] R. Meservey and P. M. Tedrow, *Phys. Rep.* **238**, 173 (1994).
- [18] Only electronic structure calculations for the whole  $\text{Co}_{80-x}\text{Fe}_xB_{20}$  range can validate this assumption. B  $s$  states in  $\text{Co}_{72}\text{Fe}_{20}\text{B}_8$  are spin polarized [3].
- [19] C. T. Chen *et al.*, *Phys. Rev. Lett.* **75**, 152 (1995).
- [20] B. T. Thole, P. Carra, F. Sette, and G. van der Laan, *Phys. Rev. Lett.* **68**, 1943 (1992).
- [21] P. Söderlind, O. Eriksson, B. Johansson, R. C. Albers, and A. M. Boring, *Phys. Rev. B* **45**, 12911 (1992).
- [22] O. Eriksson, A. M. Boring, R. C. Albers, G. W. Fernando, and B. R. Cooper, *Phys. Rev. B* **45**, 2868 (1992).
- [23] H. Ebert, R. Zeller, B. Drittler, and P. H. Dederichs, *J. Appl. Phys.* **67**, 4576 (1990).
- [24] P. Carra, B. T. Thole, M. Altarelli, and X. Wang, *Phys. Rev. Lett.* **70**, 694 (1993).
- [25] K. Fleury-Frenettea *et al.*, *J. Magn. Magn. Mater.* **220**, 45 (2000).
- [26] F. J. Himpsel, *Phys. Rev. Lett.* **67**, 2363 (1991).
- [27] C. T. Chen, N. V. Smith, and F. Sette, *Phys. Rev. B* **43**, 6785 (1991).
- [28] I. Orue, M. L. Fdez-Gubieda, and F. Plazaola, *J. Non-Cryst. Solids* **287**, 75 (2001).